


# Velocity Variation Effect in Fixed Bed Columns: A Case Study of CO<sub>2</sub> Capture Using Porous Solid Adsorbents

Nadeen Al-Janabi, Reza Vakili, Patthadon Kalumpasut, Patricia Gorgojo,  
 Flor R. Siperstein, and Xiaolei Fan   
 School of Chemical Engineering and Analytical Science, The University of Manchester,  
 Oxford Road, Manchester, U. K.

Paschal McCloskey  
 MOF Technologies Limited, 63 University Road, Belfast BT7 1NF, U. K.

DOI 10.1002/aic.16135

Published online March 8, 2018 in Wiley Online Library (wileyonlinelibrary.com)

*This study shows that for a reliable evaluation of porous adsorbents for carbon capture based on the fixed bed adsorption analysis, one must consider the effect of velocity variation due to adsorption to make a fair judgment on predicting the performance of materials under flow conditions. A combined experimental and numerical study of CO<sub>2</sub>/N<sub>2</sub> adsorption in fixed beds using three forms of adsorbents of amorphous powder (bulk activated carbon, AC), crystalline powder (bulk CuBTC metal-organic framework, MOF) and crystalline pellets (pelleted CuBTC) was carried out to show the effect of velocity variation on CO<sub>2</sub> breakthrough curves. Significant deviations are observed in the estimated amount adsorbed calculated from fixed bed experiments when models used for interpretation the measured data consider constant gas velocity because the stoichiometric time is underestimated. We show that the difference in breakthrough times estimated in models that consider constant and variable gas velocity grows exponentially with the feed gas concentration. © 2018 The Authors AICHE Journal published by Wiley Periodicals, Inc. on behalf of American Institute of Chemical Engineers AICHE J, 64: 2189–2197, 2018*

*Keywords: velocity variation, fixed bed adsorption, activated carbon, CuBTC metal organic frameworks, modeling*

## Introduction

Annually, worldwide carbon dioxide (CO<sub>2</sub>) emissions, which are related with the energy sectors, increase at a rate of *ca.* 2.1%.<sup>1</sup> This imposes a significant concern over the effort to combat the global warming. Various solutions have been proposed to achieve the goal of CO<sub>2</sub> abatement, such as the development of sustainable energy from renewable sources (e.g., biomass and solar) and carbon capture.<sup>2,3</sup> CO<sub>2</sub> capture, especially for the postcapture technology, is a very promising option as it can be easily integrated with the current industry's infrastructure, providing an immediate solution to emissions control.

The current and most widely used method for CO<sub>2</sub> capture is amine-based absorption, which suffers from intensive energy requirements for the solvent regeneration and equipment corrosion problems.<sup>4</sup> Adsorption-based separation processes using porous solids are attractive alternatives due to their lower energy regeneration requirements compared to

amine-based absorption processes. For example, in adsorption process, the heating of large amounts of water is not required during the regeneration step reducing the energy requirements.<sup>5</sup> Pressure swing adsorption (PSA) and temperature swing adsorption (TSA) have both been evaluated as feasible for large-scale CO<sub>2</sub> capture.<sup>6–10</sup> Choosing the appropriate adsorbent with high CO<sub>2</sub> selectivity, adsorption capacity, good regenerability and stability under process operating conditions, is an important factor for meeting the requirement of CO<sub>2</sub> separation for any adsorption process.<sup>11</sup>

The evaluation of the appropriateness of an adsorption process and the associated adsorbent is usually conducted experimentally complemented by mathematical modeling, to yield results that inform the design and optimization of processes. Models are useful tools to understand a process and explore wider operations windows than what is feasible to do experimentally, saving time and cost for process development and optimization. Numerical simulations require a precise analysis of the system, with careful attention to appropriate boundary conditions and assumptions contained in the model.

Mathematical models are widely used for the understanding the dynamic behavior of fixed bed column as well as the optimization of processes. They are commonly used to (i) explore the adsorption kinetics; (ii) understand the transport phenomena; (iii) estimate species distribution and temperature profiles along the fixed bed; and (iv) study the effect of process parameters (e.g., bed length, adsorption temperature, total gas flow

Additional Supporting Information may be found in the online version of this article.

Correspondence concerning this article should be addressed to X. Fan at xiaolei.fan@manchester.ac.uk and F. R. Siperstein at flor.siperstein@manchester.ac.uk

This is an open access article under the terms of the Creative Commons Attribution-NonCommercial License, which permits use, distribution and reproduction in any medium, provided the original work is properly cited and is not used for commercial purposes.

© 2018 The Authors AICHE Journal published by Wiley Periodicals, Inc. on behalf of American Institute of Chemical Engineers

**Table 1. Overview of Selected Modeling Studies of Carbon Dioxide Separation from Gas Mixtures Using Fixed Beds**

Reference	Assumptions	Comments
12	<ul style="list-style-type: none"> <li>- Bilinear driving force (bi-LDF) approximation for diffusion in micro and macro pores</li> <li>- Variable velocity</li> <li>- Appreciation of mass, energy and momentum balances</li> </ul>	<ul style="list-style-type: none"> <li>- Layered zeolite (0.8 mm)/carbon molecular sieve 3K (0.9 mm)</li> <li>- CO<sub>2</sub>/CH<sub>4</sub>/N<sub>2</sub> mixture (20% CO<sub>2</sub>, 20% CH<sub>4</sub>, 2.5 bar)</li> <li>- Effect of the ratio of adsorbent layers on the purification of methane from N<sub>2</sub> and CO<sub>2</sub> and continuous separation of CO<sub>2</sub> from N<sub>2</sub> was studied</li> </ul>
13	<ul style="list-style-type: none"> <li>- bi-LDF</li> <li>- Variable velocity</li> <li>- Appreciation of mass, energy and momentum balances</li> </ul>	<ul style="list-style-type: none"> <li>- Activated carbon (AC, 1.17 mm)/zeolite (0.85 mm), staged column with 0.5 m AC bed and 0.5 m zeolite bed</li> <li>- CO<sub>2</sub>/H<sub>2</sub>/N<sub>2</sub>/CH<sub>4</sub>/CO mixtures (7 bar)</li> <li>- Effect of the dual bed configuration on the process efficiency (e.g., purity) was studied</li> </ul>
14	<ul style="list-style-type: none"> <li>- Local equilibrium (LE) assumption</li> <li>- Isothermal condition</li> <li>- Negligible pressure drop</li> <li>- Variable velocity</li> </ul>	<ul style="list-style-type: none"> <li>- MOF-74, 177, NaX, CuBTri, BeBTB, CoBDP</li> <li>- CO<sub>2</sub>/CH<sub>4</sub>/H<sub>2</sub> (20% CO<sub>2</sub>, 0–60 bar)</li> <li>- Evaluation of MOFs and zeolite for gas adsorption in fixed bed</li> <li>- The effect of breakthrough time on the selectivity and working adsorption capacity was determined</li> </ul>
15	<ul style="list-style-type: none"> <li>- Linear driving force approximation (LDF)</li> <li>- Nonadsorbable N<sub>2</sub></li> <li>- Variable velocity</li> </ul>	<ul style="list-style-type: none"> <li>- Zeolite 13X pellets (1.03 mm)</li> <li>- CO<sub>2</sub>/N<sub>2</sub> mixture (10% CO<sub>2</sub>, 4–6.5 bar)</li> <li>- Breakthrough and heat effect of gas mixture were studied at various feed flow rates</li> </ul>
16	<ul style="list-style-type: none"> <li>- LDF</li> <li>- Variable velocity</li> <li>- Appreciation of mass, energy and momentum balances</li> </ul>	<ul style="list-style-type: none"> <li>- Zeolite 13X particles (1.6–2.6 mm)</li> <li>- CO<sub>2</sub>/N<sub>2</sub> mixture (20–60% CO<sub>2</sub>, 1 bar)</li> <li>- Empirical model combines linear and quadratic driving force was proposed</li> <li>- Heat-transfer and mass-transfer coefficients, breakthrough curves, temperature profile and mole fraction of CO<sub>2</sub> along bed were simulated</li> </ul>
17	<ul style="list-style-type: none"> <li>- LDF</li> <li>- Variable velocity</li> <li>- Appreciation of mass, energy and momentum balances</li> </ul>	<ul style="list-style-type: none"> <li>- CuBTC MOF pellets (13 mm)</li> <li>- CO<sub>2</sub>/CH<sub>4</sub>/N<sub>2</sub> (10 and 24% CO<sub>2</sub>, 2–8 bar)</li> <li>- Effect of temperature on the equilibrium selectivity was studied</li> <li>- Mass-transfer mechanism (molecular diffusion and external film resistance) was discussed.</li> <li>- Breakthrough curves for all gases with temperature profiles along the column were determined</li> </ul>
18	<ul style="list-style-type: none"> <li>- LDF</li> <li>- Variable velocity</li> <li>- Appreciation of mass, energy and momentum balances</li> </ul>	<ul style="list-style-type: none"> <li>- CuBTC MOF (1.5 mm)</li> <li>- CO<sub>2</sub>/H<sub>2</sub>/CH<sub>4</sub>/CO/N<sub>2</sub> mixtures (18–28% CO<sub>2</sub>, 2 bar)</li> <li>- 14 cycles of PSA adsorption and desorption were performed to study the performance of the adsorbent</li> <li>- Breakthrough curves for all gases with temperature profiles along the column were determined</li> </ul>
4	<ul style="list-style-type: none"> <li>- Isothermal condition</li> <li>- LE assumption</li> <li>- Constant velocity</li> </ul>	<ul style="list-style-type: none"> <li>- Cr-MIL-101</li> <li>- CO<sub>2</sub>/N<sub>2</sub> (10% CO<sub>2</sub>)</li> <li>- The effect of flue gas contamination (H<sub>2</sub>O, NO, and SO<sub>2</sub>) on CO<sub>2</sub> adsorption capacity was studied</li> <li>- Flue gas contamination was found to have minimal impact on CO<sub>2</sub> adsorption capacity</li> </ul>
19	<ul style="list-style-type: none"> <li>- Isothermal condition</li> <li>- LDF</li> <li>- Variable velocity</li> <li>- Negligible pressure drop</li> </ul>	<ul style="list-style-type: none"> <li>- Zr-based MOFs, zeolite 5A (0.85 mm) and Calgon PCB (1.17 mm)</li> <li>- CO<sub>2</sub>/H<sub>2</sub>/CH<sub>4</sub>/CO/N<sub>2</sub> mixtures (16% CO<sub>2</sub>, 7 bar)</li> <li>- Layered bed of AC and MOF was studied</li> <li>- Micropores/macropores ratio was compared to determine the dominating resistance</li> </ul>
20	<ul style="list-style-type: none"> <li>- Isothermal condition</li> <li>- Negligible pressure drop</li> <li>- Constant velocity</li> <li>- Nonadsorbable N<sub>2</sub></li> <li>- Negligible effect of external mass transfer</li> </ul>	<ul style="list-style-type: none"> <li>- AC and modified-AC (<math>d_p = 0.65</math> mm)</li> <li>- CO<sub>2</sub>/N<sub>2</sub> mixture (15% CO<sub>2</sub>, 1 bar)</li> <li>- Comparison of the breakthrough curves</li> <li>- Different kinetic models were compared and the effect of temperature and flow rate on the breakthrough profile was studied</li> </ul>
1	<ul style="list-style-type: none"> <li>- Isothermal condition</li> <li>- LDF</li> <li>- Constant velocity</li> <li>- Nonadsorbable N<sub>2</sub></li> </ul>	<ul style="list-style-type: none"> <li>- K based sorbent (K<sub>2</sub>CO<sub>3</sub>/MgO/Al<sub>2</sub>O<sub>3</sub>, 0.25–0.4 mm)</li> <li>- CO<sub>2</sub>/N<sub>2</sub>/H<sub>2</sub>O mixtures (15% CO<sub>2</sub>, 10% H<sub>2</sub>O, 0–3 bar)</li> <li>- Several equilibrium models were compared</li> <li>- Influence of mass transfer steps on predicted breakthrough curves was discussed</li> </ul>

rate, and concentration of gases in the feed) on the performance of the bed, as shown in Table 1. They can be used to assess the temperature profile and breakthrough curves for a target gas in a mixture. Assumptions often considered include isothermal operation, negligible pressure drop and mass transfer effects, and constant velocity. The choice of specific assumptions mainly depends on the computational effort needed to solve the problem and the accuracy of simulated results. Nevertheless, the validity of these assumptions needs to be considered carefully. A common assumption, valid for trace adsorption or systems with negligible pressure drop, is

that of constant velocity across the bed,<sup>21,22</sup> but its validity is questionable for separation processes where the concentration of the adsorbable component is significant or when pressure drop is not negligible. The assumption of constant velocity may result in the incorrect estimation of the propagation velocity and breakthrough curves. Zwiebel<sup>22</sup> showed that considering velocity variations due to pressure drop improves the agreement with experimental data by 5–10%, especially in the tail end of the breakthrough curves. Nevertheless, models assuming constant velocity have been used to describe CO<sub>2</sub> separation from mixtures (15–25% CO<sub>2</sub> in CO<sub>2</sub>/N<sub>2</sub> mixtures),

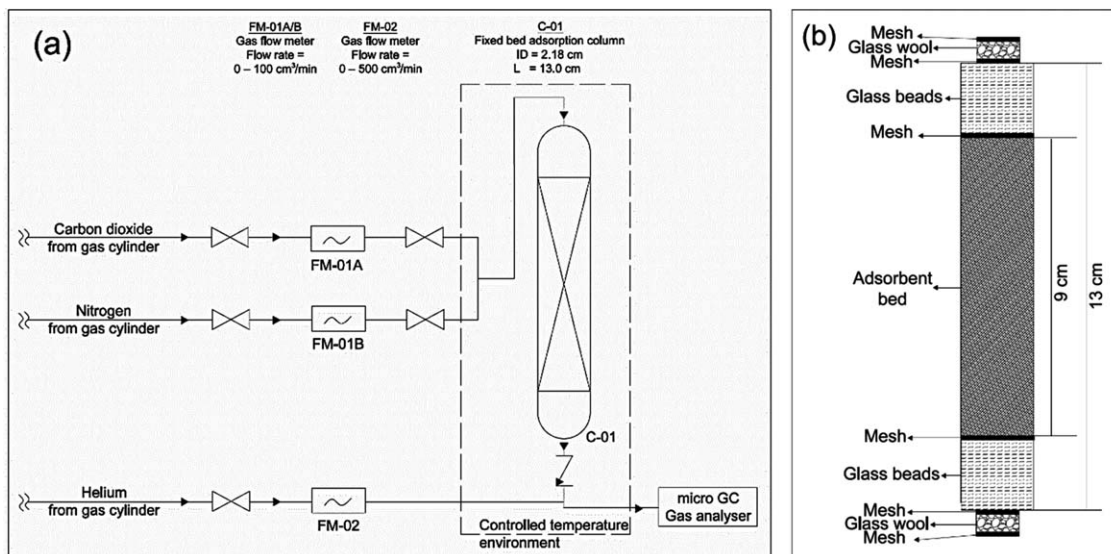


**Figure 1. (a) Schematic diagram of the fixed bed adsorption system used in this work; (b) Details of the packed bed.**

with  $<2\text{--}9.5\%$  differences<sup>20,23</sup> compared to the experimentally measured breakthrough curves. These deviations have been attributed to errors associated with the experimental procedure or model parameters estimation. From an objective point of view, the difference between the model and the measured data also likely arose from the model limitations such as the variable velocity effect during the adsorption, which was neglected in the assumption of constant propagation velocity.

Interpretation of experimental data and predictions from modelling adsorption columns may be affected by the assumptions made in the selected models. Considering that the desired purity of  $\text{CO}_2$  ( $y_{\text{CO}_2,e}$ ) to be transported or sequestered needs to be more than 95%,<sup>24</sup> the variation of propagation velocity across the fixed bed column deserves a thorough investigation to understand the criteria of setting appropriate velocity assumptions for different scenarios. In this study, the effect of propagation velocity on the breakthrough curves was studied both experimentally and numerically using a wide range of  $\text{CO}_2$  composition in  $\text{CO}_2/\text{N}_2$  mixture (0.5–80%). Fixed bed adsorption experiments were carried out using materials with different properties and working capacities, that is, bulk activated carbon (AC), bulk CuBTC (BTC = benzene-1,3,5-tricarboxylate) and pelleted CuBTC, to show the effect of velocity variation caused by different adsorbents. Crystalline CuBTC MOF was selected in this work because it is a well-studied MOF with good thermal stability (up to  $310^\circ\text{C}$ )<sup>25</sup> and available commercially at scale.<sup>26</sup>  $\text{CO}_2$  adsorption on the economical amorphous AC was used as the benchmark case to demonstrate the ability of using MOFs for practical  $\text{CO}_2$  capture.

## Materials and Experimental Method

### Materials and characterization

Activated carbon (bulk AC, *ca.*  $150\ \mu\text{m}$ ) and glass beads ( $212\text{--}300\ \mu\text{m}$ ) were purchased from Sigma Aldrich. Bulk ( $100\text{--}200\ \mu\text{m}$ ) and pelleted (1 mm diameter and *ca.* 8 mm length) CuBTC MOFs were obtained from MOF Technologies Ltd. All materials were used as received without further purification. Several characterization techniques were used to assess the properties of AC and CuBTC including powder x-ray diffraction

(PXRD) and nitrogen ( $\text{N}_2$ ) adsorption at  $-196^\circ\text{C}$  and gravimetric adsorption analysis using pure  $\text{CO}_2$  and  $\text{N}_2$  at  $50^\circ\text{C}$  using the Intelligent Gravimetric Analyser (IGA). Details of the analytical apparatus and procedure can be found elsewhere.<sup>25</sup>

### Fixed bed adsorption experiments and breakthrough measurements

The adsorption experiments and breakthrough curves were measured using the experimental rig shown in Figure 1a. The adsorption system was composed of a single fixed bed column, mass flow controllers, and a microgas chromatography (GC). To avoid the flow maldistribution caused by the bed settling,<sup>27</sup> the fixed bed column was positioned vertically with the feed gas flowing downward through the bed. The feed gas flow rates ( $\text{CO}_2$ ,  $\text{N}_2$ , and helium) were controlled by mass flow controllers (Alicat scientific MC-series,  $\pm 5\%$  accuracy). The relative  $\text{CO}_2$  feed composition was regulated by varying the flow rate of  $\text{CO}_2$  and  $\text{N}_2$ . The flow rate of  $\text{CO}_2$  was always kept at the lowest allowable value ( $5\ \text{cm}^3/\text{min}$ ) to avoid the fast saturation of adsorption bed by  $\text{CO}_2$  and the collection of quality experimental data points.

The bed outlet stream was diluted with helium (He,  $475\ \text{cm}^3/\text{min}$ ) before it was directed in to the micro GC (Agilent technologies 490 Micro GC) with a PoraPlot U (PPU) column and a thermal conductivity detector (TCD) for in-line analysis of outlet gases. The fixed bed column and the inlet piping were placed inside an oven (Mettler) to ensure the system was isothermal for the adsorption experiments. All experiments were carried out at a constant temperature of  $50^\circ\text{C}$ , simulating the emission temperature of flue gases,<sup>25</sup> and the packed materials were first activated overnight at  $200^\circ\text{C}$  under vacuum. Then, they were activated *in situ* at  $100^\circ\text{C}$  under He ( $500\ \text{cm}^3/\text{min}$ ) for two hours prior to the adsorption measurements. The pressure drop across the fixed bed was measured using a differential pressure meter (Kane 3200), as well as determined using the pressure reading from the mass flow controllers at inlet and outlet of the fixed bed column. Under the conditions used in this study, the pressure drop was found to be directly proportional to the overall flow rate with a maximum value of about 4 mbar/m (Supporting Information Figure S3a). For each experiment, fresh adsorbents were

**Table 2. Properties of Fixed Bed Column and Input Parameters**

Column length	13 cm
Bed length ( $L$ )	9 cm
Bed diameter ( $D$ )	2.18 cm
Temperature ( $T$ )	50°C
Inlet pressure ( $P_0$ )	1–1.5 bar
Void fraction ( $\varepsilon$ )	0.31 for bulk AC and CuBTC MOF 0.56 for CuBTC MOF pellets
Particle diameter ( $d$ )	0.15 mm for AC 0.10 mm for bulk CuBTC 1.0 mm for pelleted CuBTC
Total flow rate ( $F$ )	10–100 cm <sup>3</sup> /min

always used and materials were cleaned offsite at 200°C under vacuum prior to their packing in the column.

The adsorbent (13–15 g, no dilution) was packed in a stainless steel column (total length = 13 cm, internal diameter = 2.18 cm). In this work, the ratio of bed diameter to particle diameter ( $D/d$ ) were estimated as >140 for bulk AC and CuBTC. Where for CuBTC pellets, the ratio of  $D/d$  was about 22. These ratios are sufficient to avoid problems of channeling and radial dispersion.<sup>27,28</sup> A ratio of  $D/d > 100$  necessary to promote intermixing of flow streams near wall and central region<sup>27</sup> is only achieved for the columns containing bulk AC and bulk CuBTC MOF. The properties of the fixed bed column are given in Table 2.

The configuration of the column is shown in Figure 1b, inert layers of glass beads were used to support the adsorbent bed in the column and they were separated from the adsorbent bed with fine meshes to prevent the mixing of glass beads with the adsorbent.<sup>27</sup> The inert regions facilitate the flow distribution as well as act as the ballast to prevent the movement of adsorbents, and hence their attrition. The inert glass beads were bigger than the size of adsorbent particles (212–300  $\mu\text{m}$ ) to avoid pressure drop.<sup>27</sup> Glass wool layers were placed at the inlet and outlet of the column to prevent the possible migration of the ballast through the inlet and outlet tubes. The bed void fraction was determined using the correlation chart presented in the reference,<sup>29</sup> where the void fraction was given as a function of the ratio of particle to tube diameter depending on the morphology of particles. A flow rate range of 10–100 cm<sup>3</sup>/min was used in this work. Prior to the experiments, blank experiments were performed using a bed consisting of non-CO<sub>2</sub> adsorbing glass beads to estimate the gas-solid contact time, which is < 2 min (Supporting Information Figure S3b).

### Theoretical aspects

A general mathematical model that describes the dynamics of CO<sub>2</sub> adsorption in the fixed bed assuming: (i) ideal gas, (ii) isothermal condition across the bed, (iii) negligible N<sub>2</sub> adsorption compared to CO<sub>2</sub>, and (iv) negligible radial and axial dispersion is shown in Eqs. 1–3.<sup>21</sup>

Component mass balance

$$\varepsilon \frac{\partial C_i}{\partial t} + \frac{\partial(uC_i)}{\partial z} + (1-\varepsilon)\rho_g \frac{\partial q_i}{\partial t} = 0 \quad (1)$$

Ergun equation for computing the pressure drop across the bed

$$-\frac{\partial P}{\partial z} = 150 \frac{\mu_g(1-\varepsilon)^2}{\varepsilon^3 d^2} u + 1.75 \frac{(1-\varepsilon)}{\varepsilon^3 d} \rho_g u^2 \quad (2)$$

The concentration of specific component in the mixture ( $C_i$ ) is given by

$$C_i = \frac{y_i P}{RT} \quad (3)$$

The rate of adsorption can be described using different approximations: the local equilibrium (LE) assumption (Eq. 4) considers the negligible mass transfer resistance through the adsorbent particles, and the linear driving force (LDF) model (Eq. 5) assumes that the adsorption rate is proportional to a linear gradient between the average amount adsorbed in the particle, and the amount adsorbed at the surface of the particle (in equilibrium with the bulk concentration)

$$\frac{\partial q_i}{\partial t} = \frac{\partial q_i^*}{\partial t} \quad (4)$$

$$\frac{\partial \bar{q}_i}{\partial t} = k_i (q_i^* - \bar{q}_i) \quad (5)$$

where  $k_i$  is the overall resistance to mass transfer,  $q_i^*$  is the adsorbed amount at equilibrium given by the adsorption isotherm  $q_i^* = f(C, T)$ , and  $\bar{q}_i$  is the average adsorbed amount.

Assuming constant velocity throughout the bed, Eq. 1 is simplified to

$$\varepsilon \frac{\partial C_i}{\partial t} + u \frac{\partial C_i}{\partial z} + (1-\varepsilon)\rho_g \frac{\partial q_i}{\partial t} = 0 \quad (6)$$

Nevertheless, this assumption is only valid for trace amounts adsorbed. When the adsorbate concentration is high in the feed gas, the velocity of the gas will change as gas molecules are adsorbed on the adsorbent. In this case, if the column operates at constant feed pressure, the overall mass balance shown in Eq. 6 is given by

$$C \frac{\partial u}{\partial z} + (1-\varepsilon)\rho_g \frac{\partial q_i}{\partial t} = 0 \quad (7)$$

Combining Eq. 1 with Eq. 7, and assuming that only one component is adsorbed, the behavior of the column is described by

$$\varepsilon \frac{\partial C_i}{\partial t} + u \frac{\partial C_i}{\partial z} - y_i(1-\varepsilon)\rho_g \sum_{i=1}^n \frac{\partial q_i}{\partial t} + (1-\varepsilon)\rho_g \frac{\partial q_i}{\partial t} = 0 \quad (8)$$

The boundary conditions for an unused bed are:  $t = 0, P = P_0, C_i(z, 0) = q_i(z, 0) = 0$ . The model was coded numerically in MATLAB 8.3 (R2014a). Individual component and overall material balances were converted from the partial differential equation (PDE) into sets of ordinary differential equations (ODEs) by the discretization of the derivative term with respect to length of the bed. The resulting ODE system, which was subjected to initial boundary conditions of the breakthrough process, was integrated with respect to time using MATLAB ODE15s solver. The integration was performed with dividing the bed into 40 equal length segments ( $z$ ) with 1 s time step.

An analytical solution developed by Bohart and Adams (denoted as B-A model, Eq. 9)<sup>30</sup> was used in this work to validate the implementation of the model with constant velocity and LDF assumptions. The breakthrough curve in the B-A model is given by

$$\frac{C}{C_0} = \frac{\exp(k' C_0 (t - \frac{L}{u}))}{\exp(k' C_0 (t - \frac{L}{u})) + \exp(\frac{k' q_s L}{u} (1 - \varepsilon)) - 1} \quad (9)$$

The expression in Eq. 9 can be simplified when  $t \gg L/u$  as proposed by Cooney<sup>31</sup>

$$\frac{C}{C_0} = \frac{1}{1 + \exp(k' (q_s(1-\varepsilon)\frac{L}{u} - C_0 t))} \quad (10)$$

Equation 10 was linearized considering  $[\ln(C_0/C - 1)]/C_0$  as a function of time ( $t$ ) to obtain  $k'$  from the experimental data.<sup>32</sup>

## Results and Discussion

### Model validation and parametric study

The effects of constant and variable velocity assumptions on calculated breakthrough curves were studied for an activated carbon column where the total pressure was 1 bar. The system was assumed to behave as an ideal gas, with a gas viscosity of  $16.13 \times 10^{-6}$  Pa.s at 1 bar.<sup>33</sup> The Langmuir isotherm was used to fit the experimental data of CO<sub>2</sub> adsorption on activated carbon, with parameters given in the Supporting Information. The rate constants for the B-A model were obtained from experimentally measured breakthrough curves (see Supporting Information). The B-A model assumes constant fluid velocity through the bed,<sup>32</sup> and it was found previously to be capable of predicting the breakthrough behavior of solid adsorbents for CO<sub>2</sub> separation for the purpose of scaling up.<sup>34</sup>

We found that there is a significant difference between the breakthrough curves when velocity is considered constant or variable for both rate of adsorption models: LE and LDF when a CO<sub>2</sub> feed gas concentration of 50% is considered (Figure 2). Figure 2a shows the results for the LE model where the time at which  $C/C_0 = 0.5$  (that we refer to as  $t_{b50}$ ) in the curves for constant velocity coincides with the B-A model (Supporting Information Table S1). Figure 2b shows that the numerical solution using the LDF model agrees with the B-A model, validating the implementation of equations to describe the column dynamics.

The breakthrough curves assuming the local equilibrium approximation (Figure 2a) are significantly sharper than those obtained with the LDF approximation (Figure 2b). Nevertheless, in both cases a noticeable shift is observed when considering constant or variable velocity. Experimental data can be well represented assuming the LDF model and variable velocity.

Both models for rate of adsorption show that the breakthrough time for the variable velocity model is significantly smaller than for the constant velocity model, despite using the same adsorption isotherm model in both cases. This difference in  $t_{b50}$  decreases with an increase of the flow rate, but the ratio of  $t_{b50}$  between both models is always within 15–17%. Using a simple integration of the breakthrough curve

and the feed flow rate to estimate the total amount adsorbed at equilibrium would suggest different equilibrium amounts adsorbed based on the chosen model, with a lower total amount adsorbed in the variable velocity model than in the constant velocity model.

The effect of adsorbable gas (CO<sub>2</sub>) inlet concentration on the breakthrough curves was studied by changing the N<sub>2</sub> flow rate based on a constant CO<sub>2</sub> flow rate (5 cm<sup>3</sup>/min). Results for experiments performed using three adsorbents of bulk AC, bulk CuBTC and pelleted CuBTC MOFs are presented in Figure 3. A decrease in the concentration of CO<sub>2</sub> in the feed reduced the deviation between calculated constant and variable velocity breakthrough curves (both using the LDF model). It was expected because a lower concentration in the feed uptakes would move the system closer to the idealized constant velocity case that is valid only for trace adsorption. A parametric study in Figure 4 shows that the variable and constant velocity models converge at very low concentrations, supporting the statements above. It was found that the discrepancy between the two models increased exponentially with the increasing CO<sub>2</sub> composition in the feed stream, as shown in Figure 4b.

Experimental results for bulk AC and pelleted CuBTC MOF, and bulk CuBTC MOF were well described by the variable velocity LDF model (Figure 3d). Nevertheless, the breakthrough curve of CO<sub>2</sub> on bulk CuBTC MOF when the gas feed concentration was 50% showed some significant deviations from the model at long times. It is possible that heat effects due to the high heat of adsorption of CO<sub>2</sub> on CuBTC MOF played a more important role when the adsorbent is a powder.<sup>17</sup> The measured equilibrium adsorption isotherms for CO<sub>2</sub> on CuBTC MOF powder and pellets are practically identical (Supporting Information Figure S2). The  $t_{b50}$  for CO<sub>2</sub> on CuBTC MOF powder is 23 min, whereas for CO<sub>2</sub> on CuBTC pellets is 14 min, suggesting that mass transfer resistances are more important in the pellet form, and probably allowing more time for heat transfer and enabling the system to be isothermal. As the CO<sub>2</sub> concentration decreases, heat effects decrease, as expected.

### Parametric study: calculation of CO<sub>2</sub> adsorption isotherms

In the fixed bed adsorption studies, the usable capacity of the solid adsorbent is usually determined from the breakthrough

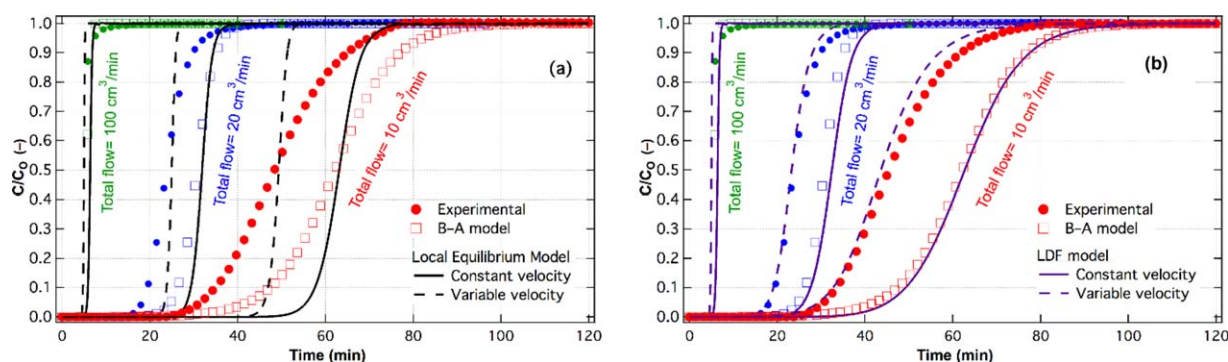


**Figure 2.** (a) Comparison of modelled breakthrough curves based on the local equilibrium theory, considering constant (solid line) or variable (dashed line) velocity at different flow rates. Solid symbols represent experimental data for adsorption of CO<sub>2</sub> on AC and open symbols represent the B-A model; (b) Comparison of modelled breakthrough curves based on the LDF theory, considering constant (solid line) or variable (dashed line) velocity at different flow rates. Solid symbols represent experimental data and open symbols represent the B-A model.

[Color figure can be viewed at [wileyonlinelibrary.com](http://wileyonlinelibrary.com)]

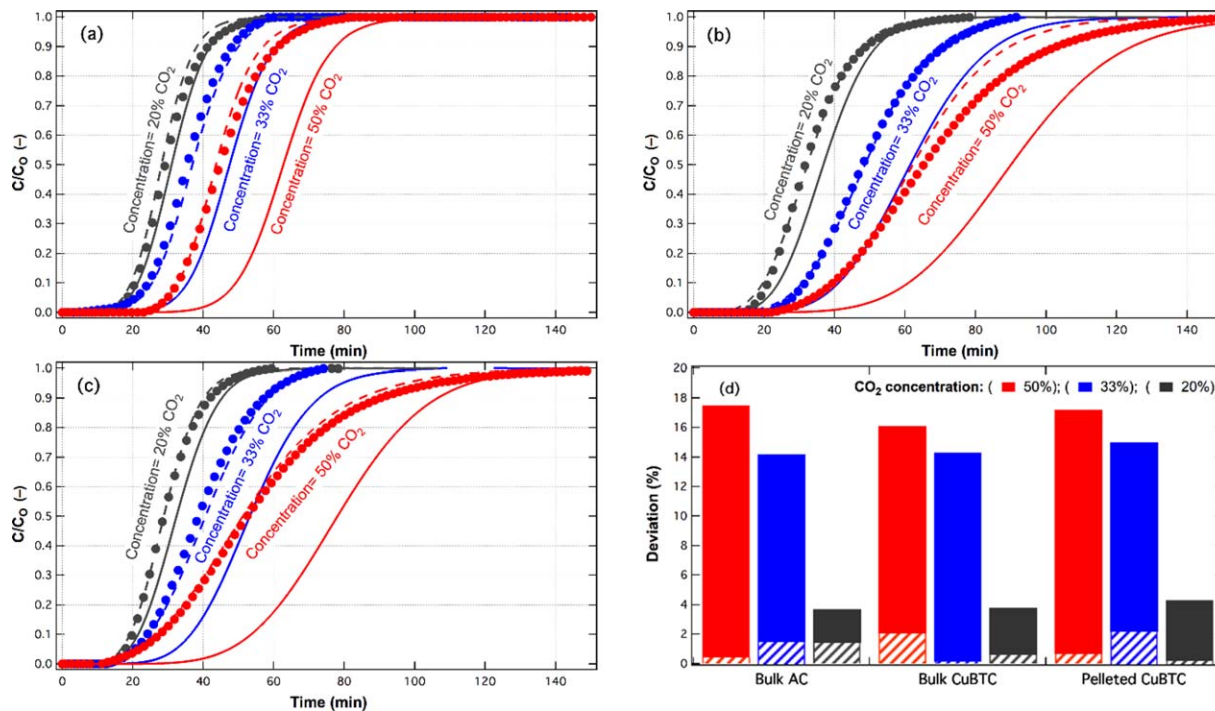


**Figure 3.** Breakthrough curves at different feed CO<sub>2</sub> concentrations (CO<sub>2</sub> = 5 cm<sup>3</sup>/min) (a) bulk AC; (b) bulk CuBTC MOF; and (c) pelleted CuBTC MOF, Solid circles represent experimental data, solid lines are the model with constant velocity assumption, and dash line are the model with variable velocity assumption; (d) deviation of  $t_{b50}$  between the experimental data, constant (solid) and variable (dashed) velocity models. [Color figure can be viewed at wileyonlinelibrary.com]

experiments by applying mass balance to the bed, as illustrated in Eq. 11

$$q_{CO_2} = \frac{y_{CO_2} F_0 C_0 t_b}{W} \quad (11)$$

where  $q_{CO_2}$  is the quantity of CO<sub>2</sub> adsorbed per unit mass of adsorbents,  $y_i$  is the CO<sub>2</sub> mole fraction in the feed,  $F_0$ , and  $C_0$  are the initial total flow rate and initial total concentration,  $W$  is the mass of adsorbent and  $t_b$  is the breakthrough time.

The amount adsorbed at equilibrium is defined as

$$q_{CO_2}^* = \frac{1}{W} \int_0^\infty (\varepsilon A u_0 C_0 - \varepsilon A u_e C_e) dt \quad (12)$$

where  $A$  is the bed cross sectional area,  $\varepsilon$  is the bed porosity,  $C_0$  and  $C_e$  are the initial feed and effluent concentrations, and  $u_0$  and  $u_e$  are the feed and effluent velocities. Assuming constant velocity and knowing that the volumetric flow rate  $F = Au$ , and concentration  $C_i = Cy_i$ , then the amount adsorbed at equilibrium can be written as

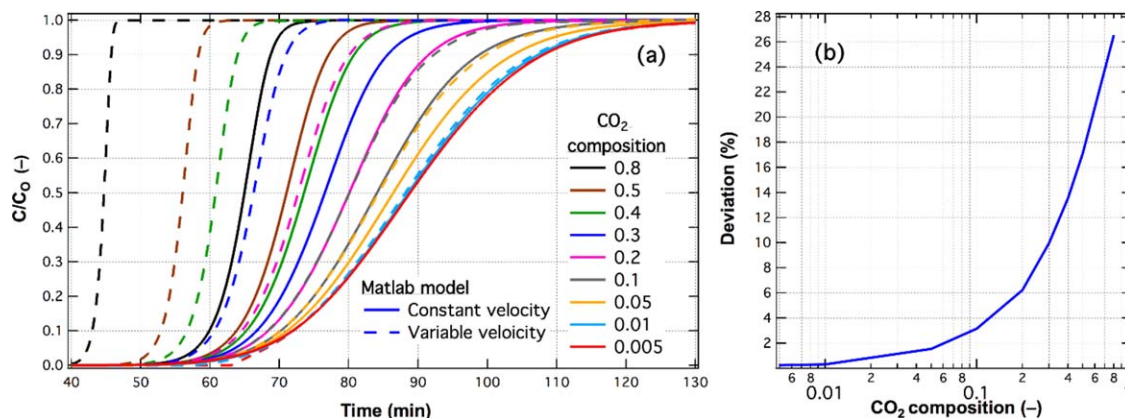


**Figure 4.** Parametric study of the effect of CO<sub>2</sub> feed concentration on the breakthrough curves considering constant and variable velocities (total flow = 10 cm<sup>3</sup>/min, total inlet pressure = 1 bar,  $T = 50^\circ\text{C}$ ).

(a) Simulated breakthrough curves by the numerical models with different velocity assumptions, solid lines (—): Numerical model with constant velocity assumption, dash line (- -): Numerical model with variable velocity assumption. (b) Deviations of  $t_{b50}$  between simulated results of numerical modes with different velocity assumptions. [Color figure can be viewed at wileyonlinelibrary.com]

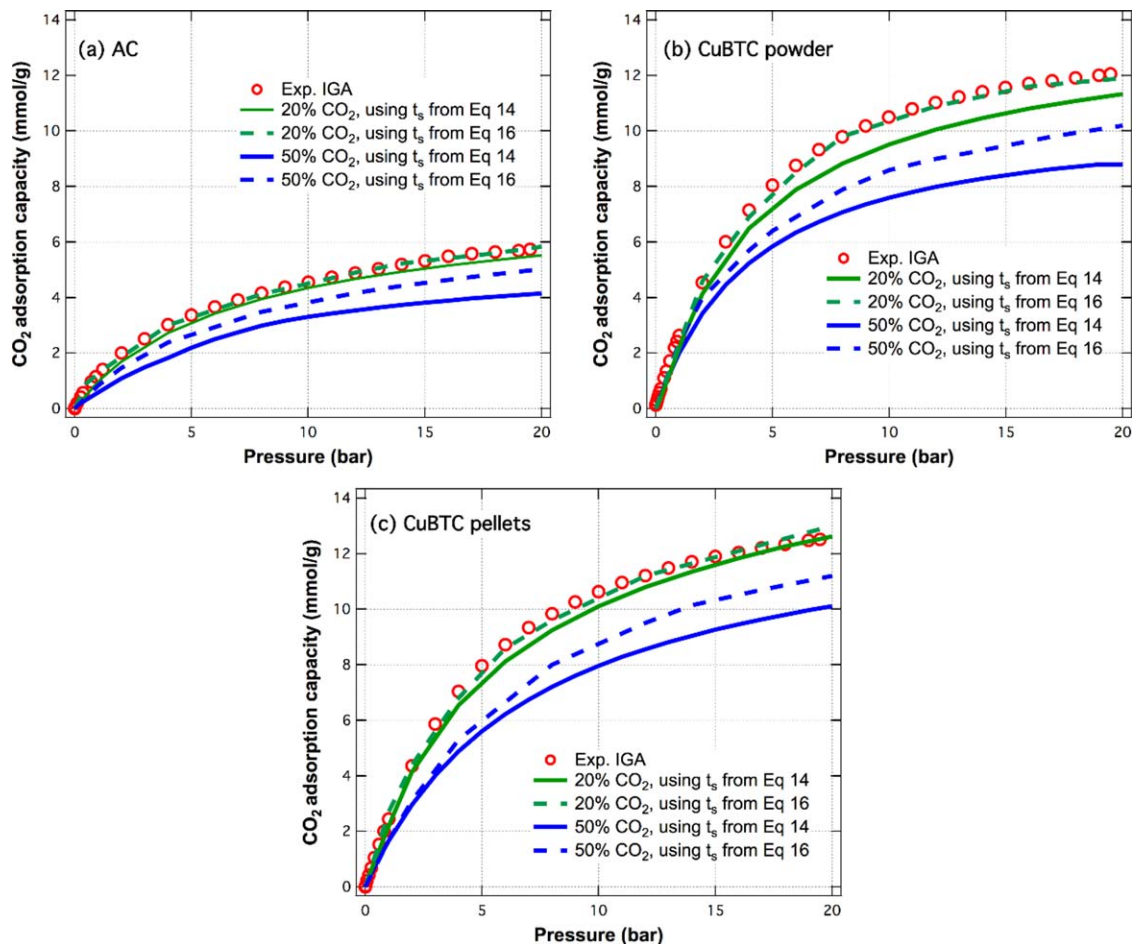


**Figure 5. Deviation in CO<sub>2</sub> adsorption isotherms at 50°C for (a) Bulk AC, (b) Bulk CuBTC MOF, (c) Pelleted CuBTC MOF when corrections for variable velocity are applied in the estimation of the total amount adsorbed.**

[Color figure can be viewed at [wileyonlinelibrary.com](http://wileyonlinelibrary.com)]

$$q_{\text{CO}_2}^* = \frac{F_0 C_0}{W} \int_0^\infty \left(1 - \frac{y_{i,e}}{y_{i,0}}\right) dt \quad (13)$$

A useful quantity to use based on Eq. 13 is the stoichiometric time  $t_s$ , which is given by

$$t_s = \int_0^\infty \left(1 - \frac{y_{i,e}}{y_{i,0}}\right) dt \quad (14)$$

Then the equilibrium amount adsorbed is calculated using by applying mass balance to the bed, Eq. 11.

However, Malek et al.<sup>35</sup> reported that due to the significant velocity difference between the inlet and exit of the column in nontrace systems, Eq. 14 may lead to incorrect estimations of the equilibrium adsorption data.<sup>35</sup> They proposed an expression of the stoichiometric time, which led to accurate estimations of the stoichiometric time when the concentration of the adsorbable component in the feed is larger than 20%

$$t_s = \int_0^\infty \left(1 - \frac{y_{i,e} (1 - y_{i,0})}{y_{i,0} (1 - y_{i,e})}\right) dt \quad (15)$$

The stoichiometric time, Eq. 15, was used to estimate the equilibrium data from the breakthrough measurements as

shown in Figure 5. The estimated equilibrium amount adsorbed, based on breakthrough measurements and Eq. 15, showed a good agreement with the equilibrium data measured gravimetrically for a gas feed composition of 20% CO<sub>2</sub>. The estimated equilibrium amount adsorbed from breakthrough measurements when the feed concentration is 50% is lower than that measured gravimetrically, however, the estimations improved when compared to the equilibrium amount adsorbed estimated using Eq. 14 (as in Figure 5).

Therefore, the results showed that the assessment of the adsorption capacity of porous materials using the breakthrough measurements might underestimate the working adsorption performance of materials under real conditions if the process parameters such as the velocity variation across the bed during the adsorption process are not considered. Simple corrections as the one proposed by Malek et al.<sup>35</sup> are only valid at moderate feed concentrations; therefore careful analysis is needed when considering separation processes where the feed concentration of the adsorbable component is large.

#### Screening of adsorbents: purity of adsorbed CO<sub>2</sub>

Several factors need to be considered for the use of adsorbents in practical CO<sub>2</sub> adsorption, such as the hydrothermal stability of CuBTC MOFs,<sup>25,36–38</sup> achievable purity, ease of regeneration, and cost. The purity of separated CO<sub>2</sub> is an important factor that reflects the efficiency of adsorption

**Table 3. Minimum Working Capacity and Purity of Adsorbed CO<sub>2</sub> Determined Using Eqs.14 and 16 Based on Fixed Bed Breakthrough Curves for CO<sub>2</sub> Feed Concentration of 20%**

Adsorbent	Adsorption Capacity Measured Gravimetrically and Calculated Based on Breakthrough Curves Using Eq. 15		Adsorption Capacity Calculated Based on Breakthrough Curves Using Eq. 14	
	$\Delta q_{\min,CO_2}$ (mmol/g)	$y_{CO_2,e}$ (%)	$\Delta q_{\min,CO_2}$ (mmol/g)	$y_{CO_2,e}$ (%)
Bulk activated carbon	0.242	90.9	0.167	87.5
Bulk CuBTC	0.496	96.7	0.337	95.4
Pelleted CuBTC	0.479	95.1	0.329	92.9

processes. The purity of the separated CO<sub>2</sub> ( $y_{CO_2,e}$ ), as defined by Eq. 16, needs to be more than 95% for subsequent transportation and sequestration.<sup>24</sup> The value of  $y_{CO_2,e}$  can be estimated based on the adsorption isotherms and it should be considered in the screening of adsorbents for CO<sub>2</sub> capture

$$y_{CO_2,e} = \frac{\Delta q_{\min,CO_2} \rho_g (1-\varepsilon) + y_{CO_2,0} \frac{\varepsilon P_{feed}}{RT}}{\Delta q_{\min,CO_2} \rho_g (1-\varepsilon) + \frac{\varepsilon P_{feed}}{RT}} > 0.95 \quad (16)$$

where  $\Delta q_{\min,CO_2}$  is the minimum working capacity (mol/kg), that is, the difference of adsorption capacity between the highest and lowest working CO<sub>2</sub> partial pressures;<sup>11</sup>  $\rho_g$  is the particle density (kg/m<sup>3</sup>);  $\varepsilon$  is the void fraction of the adsorption column;  $P_{feed}$  is the pressure of the feed (Pa); and  $T$  is the temperature of the feed (K).

The purity of CO<sub>2</sub> has been estimated for the adsorbents used in this work based on a model flue gas (total pressure = 1 bar, temperature = 50°C, and CO<sub>2</sub> composition = 20%). The minimum working capacity ( $\Delta q_{\min,CO_2}$ ) was calculated based on the CO<sub>2</sub> partial pressures 0 and 0.2 bar CO<sub>2</sub> from the isotherms (both gravimetrically measured and obtained from the analysis of the fixed bed adsorption experiments), as shown in Table 3.

Based on gravimetric equilibrium data and fixed bed adsorption experiments for a CO<sub>2</sub> feed concentration of 20% when the velocity variation is considered, both bulk CuBTC and pelleted CuBTC MOFs showed values of  $y_{CO_2,e}$  higher than 95%, indicating that they are suitable porous materials for CO<sub>2</sub> capture. However, when the correction of adsorption capacity due to the velocity variation effect was not considered (Eq. 14), the adsorption isotherms are underestimated and the achievable purity is reduced. These results showed that an erroneous evaluation of the suitability of adsorbents for practical applications may arise if fixed bed adsorption data is not carefully modelled, which in this case means considering velocity variations.

## Conclusion

This work shows the importance of considering velocity variations when modelling fixed bed adsorption columns to accurately calculate the CO<sub>2</sub> breakthrough behavior. We showed that considering a variable velocity through the bed is necessary for correctly describing CO<sub>2</sub> capture in activated carbon, crystalline bulk CuBTC MOF and pelleted CuBTC MOF, unless a very diluted feed is considered (with CO<sub>2</sub> concentration < 1%). It should be noted that the effect of a high-pressure drop was not considered in this study, which can affect the propagation velocity,<sup>22</sup> because the difference in experimentally measured pressure drops in our system was insignificant.

This work shows that the difference between the stoichiometric time considering constant and variable velocity grows exponentially with the adsorbate concentration in the feed.

Malek et al.<sup>35</sup> suggested that the correction for variable velocity should be implemented when the feed concentration is higher than 20% for light adsorbing gases (methane and ethane on activated carbon) to have errors smaller than 2% in the equilibrium amount adsorbed.<sup>35</sup> For gases that adsorb stronger, such as CO<sub>2</sub> on activated carbon, a feed concentration of 20% results in a shift of the breakthrough time of 6%, and a deviation in the equilibrium amount adsorbed of 6%. For CO<sub>2</sub> adsorption on bulk and pelleted CuBTC, same deviations (i.e., 6%) in breakthrough curves and equilibrium amount adsorbed were observed.

In this work we show that the percentage shift in the breakthrough curves (or error in the estimation of the total amount adsorbed) is practically independent of the total flow rate or the adsorbent used, but strongly dependent on the feed concentration. Comparing to work reported in the literature,<sup>35</sup> the error in the total amount adsorbed is dependent of the gas considered.

According to these findings, the common evaluation of porous adsorbents for carbon capture based on the equilibrium adsorption using gravimetric analysis should be complemented by the fixed bed adsorption analysis, as well as other methods such as zero length column,<sup>39</sup> to make a fair judgment on predicting the performance of materials under flow conditions.

## Acknowledgments

We thank the financial support from The University of Manchester through Higher Education Innovation Funded “Knowledge and Innovation Hub for Environmental Sustainability” and the Royal Society Research Grant (reference: RG160031). NAJ thanks The Higher Committee for Education Development in Iraq (HCED) for the postgraduate research scholarship. RV acknowledges The University of Manchester President’s Doctoral Scholar Award for supporting his PhD research.

## Notation

$C$  = total concentration, mol/m<sup>3</sup>  
 $C_i$  = component concentration, mol/m<sup>3</sup>  
 $C_0$  = initial concentration, mol/m<sup>3</sup>  
 $D$  = internal column diameter, m  
 $d$  = particle diameter, m  
 $F$  = volumetric flow rate, cm<sup>3</sup>/min  
 $K$  = Henry’s constant in the Langmuir model, m<sup>3</sup>/mol  
 $k_i$  = mass transfer coefficient in the LDF equation, 1/s  
 $k'$  = mass transfer coefficient in the B-A model, 1/s  
 $L$  = total bed length, m  
 $n_s$  = saturation capacity in the Langmuir model, mmol/g  
 $P$  = total pressure, bar  
 $P_0$  = initial pressure, bar  
 $q_i$  = average adsorbed amount, mmol/g  
 $q^*$  = equilibrium adsorbed amount, mmol/g  
 $q_s$  = saturation capacity per unit volume of bed in the B-A model, mmol/g



$R$  = gas constant, Pa m<sup>3</sup>/mol K  
 $T$  = temperature, K  
 $t$  = time, min  
 $u$  = superficial velocity, m/s  
 $y_0$  = initial mole fraction,  
 $y_i$  = component mole fraction,  
 $y_e$  = effluent mole fraction,  
 $z$  = length of one segment in the fixed bed, m

### Greek letters

$\varepsilon$  = void fraction,  
 $\mu_g$  = viscosity of gas, Pa s  
 $\rho$  = density of gas, kg/m<sup>3</sup>  
 $\rho_g$  = grain density, kg/m<sup>3</sup>

### Literature Cited

- Zhang L, Yin Y, Li L, Wang F, Song Q, Zhan N, Xiao F, Wei W. Numerical simulation of CO<sub>2</sub> adsorption on K-based sorbent. *Energy Fuels*. 2016;30(5):4283–4291.
- Lackner KS. A guide to CO<sub>2</sub> sequestration. *Science*. 2003;300(5626):1677–1678.
- Grimston M, Karakoussis V, Fouquet R, Van der Vorst R, Pearson P, Leach M. The European and global potential of carbon dioxide sequestration in tackling climate change. *Clim Policy*. 2001;1(2):155–171.
- Liu Q, Ning L, Zheng S, Tao M, Shi Y, He Y. Adsorption of carbon dioxide by MIL-101(Cr): Regeneration conditions and influence of flue gas contaminants. *Sci Rep*. 2013;3:2916.
- Gibson JA, Mangano E, Shiko E, Greenaway AG, Gromov AV, Lozinska MM, Friedrich D, Campbell EEB, Wright PA, Brandani S. Adsorption materials and processes for carbon capture from gas-fired power plants: AMPGas. *Ind Eng Chem Res*. 2016;55(13):3840–3851.
- Shafeeyan MS, Daud WMAW, Shamiri A. A review of mathematical modeling of fixed-bed columns for carbon dioxide adsorption. *Chem Eng Res Des*. 2014;92(5):961–988.
- Hauchhum L, Mahanta P. Carbon dioxide adsorption on zeolites and activated carbon by pressure swing adsorption in a fixed bed. *Int J Energy Environ Eng*. 2014;5(4):349.
- Raganati F, Ammendola P, Chirone R. Effect of acoustic field on CO<sub>2</sub> desorption in a fluidized bed of fine activated carbon. *Particuology*. 2015;23:8–15.
- Ammendola P, Raganati F, Chirone R. CO<sub>2</sub> adsorption on a fine activated carbon in a sound assisted fluidized bed: thermodynamics and kinetics. *Chem Eng J*. 2017;322:302–313.
- Ammendola P, Raganati F, Chirone R. Effect of operating conditions on the CO<sub>2</sub> recovery from a fine activated carbon by means of TSA in a fluidized bed assisted by acoustic fields. *Fuel Process Technol*. 2015;134:494–501.
- Pirngruber GD, Hamon L, Bourrelly S, Llewellyn PL, Lenoir E, Guillerm V, Serre C, Devic T. A method for screening the potential of MOFs as CO<sub>2</sub> adsorbents in pressure swing adsorption processes. *ChemSusChem*. 2012;5(4):762–766.
- Cavenati S, Grande CA, Rodrigues AE. Separation of mixtures by layered pressure swing adsorption for upgrade of natural gas. *Chem Eng Sci*. 2006;61(12):3893–3906.
- Ribeiro AM, Grande CA, Lopes FVS, Loureiro JM, Rodrigues AE. A parametric study of layered bed PSA for hydrogen purification. *Chem Eng Sci*. 2008;63(21):5258–5273.
- Krishna R, Long JR. Screening metal–organic frameworks by analysis of transient breakthrough of gas mixtures in a fixed bed adsorber. *J Phys Chem C*. 2011;115(26):12941–12950.
- Mulgundmath VP, Jones RA, Tezel FH, Thibault J. Fixed bed adsorption for the removal of carbon dioxide from nitrogen: breakthrough behaviour and modelling for heat and mass transfer. *Sep Purif Technol*. 2012;85:17–27.
- Won W, Lee S, Lee K-S. Modeling and parameter estimation for a fixed-bed adsorption process for CO<sub>2</sub> capture using zeolite 13X. *Sep Purif Technol*. 2012;85:120–129.
- Najafi Nobar S, Farooq S. Experimental and modeling study of adsorption and diffusion of gases in Cu-BTC. *Chem Eng Sci*. 2012;84:801–813.
- Silva B, Solomon I, Ribeiro AM, Lee U-H, Hwang YK, Chang J-S, Loureiro JM, Rodrigues AE. H<sub>2</sub> purification by pressure swing adsorption using CuBTC. *Sep Purif Technol*. 2013;118:744–756.
- Banu A-M, Friedrich D, Brandani S, Düren T. A multiscale study of MOFs as adsorbents in H<sub>2</sub> PSA purification. *Ind Eng Chem Res*. 2013;52(29):9946–9957.
- Shafeeyan MS, Daud WMAW, Shamiri A, Aghamohammadi N. Modeling of carbon dioxide adsorption onto ammonia-modified activated carbon: Kinetic analysis and breakthrough behavior. *Energy Fuels*. 2015;29(10):6565–6577.
- Ruthven DM. *Principles of Adsorption and Adsorption Processes*. New Jersey: John Wiley & Sons, 1984.
- Zwiebel I. Fixed bed adsorption with variable gas velocity due to pressure drop. *Ind Eng Chem Fundam*. 1969;8(4):803–807.
- Sabouni R, Kazemian H, Rohani S. Mathematical modeling and experimental breakthrough curves of carbon dioxide adsorption on metal organic framework CPM-5. *Environ Sci Technol*. 2013;47(16):9372–9380.
- Farrusseng D. *Metal-Organic Frameworks: Applications from Catalysis to Gas Storage*. Weinheim: Wiley-VCH Verlag GmbH & Co. KGaA, 2011.
- Al-Janabi N, Hill P, Torrente-Murciano L, Garforth A, Gorgojo P, Siperstein FR, Fan X. Mapping the Cu-BTC metal–organic framework (HKUST-1) stability envelope in the presence of water vapour for CO<sub>2</sub> adsorption from flue gases. *Chem Eng J*. 2015;281:669–677.
- Crawford D, Casaban J, Haydon R, Giri N, McNally T, James SL. Synthesis by extrusion: continuous, large-scale preparation of MOFs using little or no solvent. *Chem Sci*. 2015;6(3):1645–1649.
- Thomas WJ, Crittenden BD. *Adsorption Technology and Design*, 2nd ed. Oxford: Butterworth-Heinemann, 1998.
- Delgado J. A critical review of dispersion in packed beds. *Heat Mass Transf*. 2006;42(4):279–310.
- Couper JR, Penney WR, Fair JR. *Chemical Process Equipment: Selection and Design*, 3rd ed. Oxford: Butterworth-Heinemann, 1990.
- Bohart GS, Adams EQ. Some aspects of the behaviours of charcoal with respect chlorine. *J Am Chem Soc*. 1920;42(3):523–544.
- Cooney DO. *Adsorption Design for Wastewater Treatment*. Florida: CRC Press, 1998.
- Chu K, Hashim M. Copper biosorption on immobilized seaweed biomass: column breakthrough characteristics. *J Environ Sci*. 2007;19(8):928–932.
- Fenghour A, Wakeham WA, Vesovic V. The viscosity of carbon dioxide. *J Phys Chem Ref Data*. 1998;27(1):31–44.
- Monazam ER, Spenik J, Shadle LJ. Fluid bed adsorption of carbon dioxide on immobilized polyethylenimine (PEI): kinetic analysis and breakthrough behavior. *Chem Eng J*. 2013;223:795–805.
- Malek A, Farooq S, Rathor MN, Hidajat K. Effect of velocity variation due to adsorption-desorption on equilibrium data from breakthrough experiments. *Chem Eng Sci*. 1995;50(4):737–740.
- Al-Janabi N, Alfutimie A, Siperstein FR, Fan X. Underlying mechanism of the hydrothermal instability of HKUST-1 metal-organic framework. *Front Chem Sci Eng*. 2016;10(1):103–107.
- Al-Janabi N, Martis V, Servi N, Siperstein FR, Fan X. Cyclic adsorption of water vapour on CuBTC MOF: sustaining the hydrothermal stability under non-equilibrium conditions. *Chem Eng J*. 2018;333:594–602.
- Al-Janabi N, Deng H, Borges J, Liu X, Garforth A, Siperstein FR, Fan X. A facile post-synthetic modification method to improve hydrothermal stability and CO<sub>2</sub> selectivity of CuBTC metal-organic framework. *Ind Eng Chem Res*. 2016;55(29):7941–7949.
- Hu X, Brandani S, Benin AI, Willis RR. Development of a semi-automated zero length column technique for carbon capture applications: rapid capacity ranking of novel adsorbents. *Ind Eng Chem Res*. 2016;54(26):7941–7949.

Manuscript received July 24, 2017, and revision received Jan. 10, 2018.